Int. J. Solids Structures Vol. 20, No. 7, pp. 699–713, 1984
Printed in the U.S.A.

0020–7683/84 $3.00 + .00
Pergamon Press Ltd.

ON THE COLLAPSE OF CIRCULAR CONFINED RINGS UNDER EXTERNAL PRESSURE

S. KYRIAKIDES and S.-K. YOUN
Department of Aerospace Engineering and Engineering Mechanics,
The University of Texas at Austin, Austin, TX 78712, U.S.A.

(*Received* 19 *August* 1983; *in revised form* 3 *October* 1983)

Abstract—The paper presents a study of the large deflection collapse of circular rings confined in a rigid cavity under external pressure. The ring is assumed to be inextensional and to have an initial localized imperfection which causes a small section of its circumference to be detached from the confining wall. The cavity formed is pressurized and its growth examined. The formulation is general enough to allow for large deflections of the ring as well as material nonlinearities.

The pressure v's change in volume response of the confined ring is found to be characterized by a limit load for both elastic and inelastic material behavior. The limit load is shown to be dependent on both the geometry of the initial imperfection as well as the yield and post yield characteristics of the ring material. The response beyond the limit load is unstable until the crown of the ring touches the opposite side after which it becomes stable again.

NOTATION

E	Young's Modulus
E'	post yield slope of multilinear σ–ϵ curve
H	horiziontal force at any point in the ring
$\bar{H}$	$6\pi HR/\sigma_0 t^2$
M	moment
$\bar{M}$	$6M/\sigma_0 t^2$
N	number of descretion
P	pressure
P	$6\pi^2 R^2 P/t^2\sigma_0$
P_c	limit pressure
R	ring radius
S	mid-plane ring coordinate
s	$S/\pi R$
S^*, s^*	S, s at ring separation point, respectively
t	ring thickness
α	E/E'
α^*	$\theta(S^*)$
β^*	defined in Fig. 6
ϵ	strain
θ_0	θ for undeformed ring
κ	curvature
κ_1	curvature at on-set of unloading
ξ	cartesian coordinate defining imperfection
σ	stress
σ_0	yield stress

INTRODUCTION

Many long, tunnel-like structures built underground are lined with thin-walled cylindrical shells. Depending on the application, the liners serve as either pressure containment vessels or as structural supports safeguarding the integrity of the circular geometry of the hole. In the applications of interest, the lining is grouted in place with cement which results in a continuous and circular cavity with which the shell is in contact. Examples of this type of structure are oil, gas, steam and water well casing[1, 2]; tunnels and ducts used in hydroelectric plants [3, 4], conventional and nuclear power plants[5, 6], etc.

In all applications mentioned, conditions can develop in which pressure builds up in the interface of the cement cavity and the liner or casing (see [7]). Usually severe enough imperfections exist that buckling of the liner can result. Many investigators have in the past

dealt with the problem of predicting the buckling pressure as a function of the imperfections. In [8, 9] the problem was idealized as a thin elastic circular ring embedded in a "smooth" rigid contacting confining cavity. Estimates of the buckling pressure as a function of the initial imperfections were obtained and design rules established. More recently, Yamamoto and Matsubara extended the results to a section of confined shell supported at the ends by bulkheads[5]. The effect of plastic deformation on the buckling load was also considered[6].

Kyriakides and Babcock, in a short reference to this class of problems[10], presented experimental evidence which indicates that long confined shells under external pressure can develop a buckle which propagates. The characteristics of this phenomenon are very similar to those of the propagating buckle experienced mainly in offshore pipelines[10, 11]. The collapse process gets initiated from a local, but substantial, dent or damage on the confined shell and driven by pressure it propagates within the confines of the cavity and can potentially destroy the whole structure. The nature of the problem is illustrated in Fig. 1 which shows a series of cross sections through which a section of the collapsed tube undergoes as it is collapsed by a propagating buckle of this type. A more detailed description of the phenomenon is given in [7].

The present study is motivated by this phenomenon. Due to the difficulties involved in pursuing a large deflection, plastic analysis of the complete confined shell, it is felt that a great deal of insight into the problem can be gained by first examining in detail the large deflection response of a thin, inelastic confined ring under external pressure. A corresponding study for the propagating buckle proved to be very successful in the past[10–15]. In what follows a thin-walled inextensional ring confined in a circular contacting cavity is considered. A local imperfection is introduced to the ring geometry by assuming part of the ring to be initially detached from the wall of the cavity. The ring is pressurized through this cavity. The problem is formulated through a large displacement formulation and solved numerically. Both elastic and inelastic material behavior for the ring are considered.

A great deal of insight into the buckling characteristics of confined rings can be gained from a review of a very rich literature on the subject. Although reference to all related works is not attempted, particular reference must be made to the works of Hsu Lo *et al.*[16] who considered the postbuckling configurations of a thermally heated confined ring; Hsu *et al.*[17], Buckiarelli and Pian[18], and Chan and McMinn[19] considered the effect of initial imperfections on the limit load type of buckling exhibited by this problem; Zagustin and Herrmann[20] presented an analytical approach to finding the response of a confined ring to a gravity type of loading. El-Bayoumy considered the same thermal problem through an energy formulation[21].

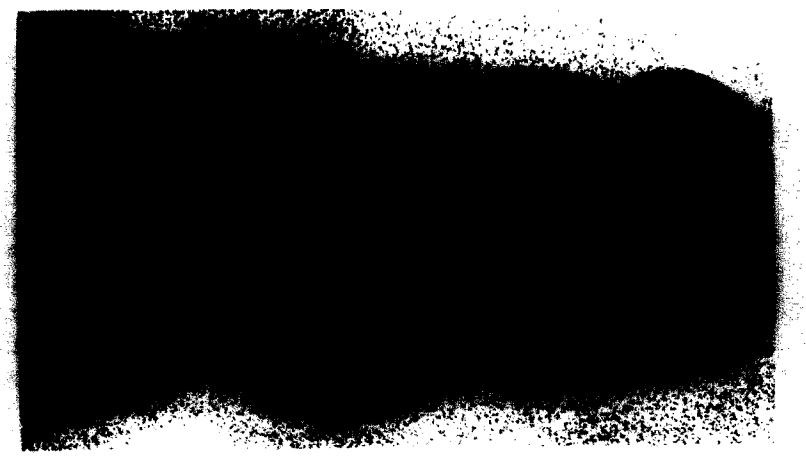

Fig. 1. Sections through profile of confined propagating buckle.

An interesting conclusion drawn by a number of these investigators (see also [22]) is that a uniformly loaded (e.g. thermal load) circular confined ring exhibits no classical bifurcation load. A limit load type of buckling (snap-through) is, however, possible with the presence of initial geometric imperfections. The limit load is a function of the geometry of the imperfection.

THE PROBLEM

We consider a thin, inextensional ring of radius R, thickness t and unit width, confined in a circular, contacting cavity (Fig. 2). In the unloaded stress-free state, the ring has a small geometric imperfection extending over a section of length $2S_0$ and having amplitude Δ_0 which causes the ring to be locally detached from the confining wall of the cavity. The imperfection is assumed to be formed inextensionally from a circle of radius R. The imperfection is symmetric about an axis through the center of the ring. The problem consists of finding the response of this ring to external pressure. The pressure is assumed to be built up inside the cavity formed between the rigid wall and the detached portion of the ring.

It is assumed that the ring deformations will remain symmetric with respect to the X-axis (Fig. 2) and, as a result, only half of the ring is considered. It is also assumed that at any given load, the ring domain is clearly divided into the detached section AB (see Fig. 3) and section BC which remains everywhere in contact to the wall. Pressure is only applied to section AB. The rigid confining wall can react to normal loads, but the contact with the ring is assumed to be frictionless.

The problem is formulated within the customary small strain and negligible shear deformations assumptions of beam theory. Geometric nonlinearities are introduced by allowing for large deflections (finite rotations).

GEOMETRY

As in all contact problems, a suitable solution procedure has to overcome the difficulty of not knowing a priori the domain of the problem. This difficulty is overcome by incrementally fixing the domain by prescribing the separated length of ring. Thus, by prescribing AB to have a length S^*, point B is also fixed to be at an angle α^* (Fig. 3).

It can easily be shown that for inextensional deformations of the detached section, the position of any point (X, Y) relative to the cartesian frame shown in Fig. 3, is described by

$$\frac{dX}{dS} = -\sin\theta, \qquad \frac{dY}{dS} = \cos\theta, \tag{1}$$

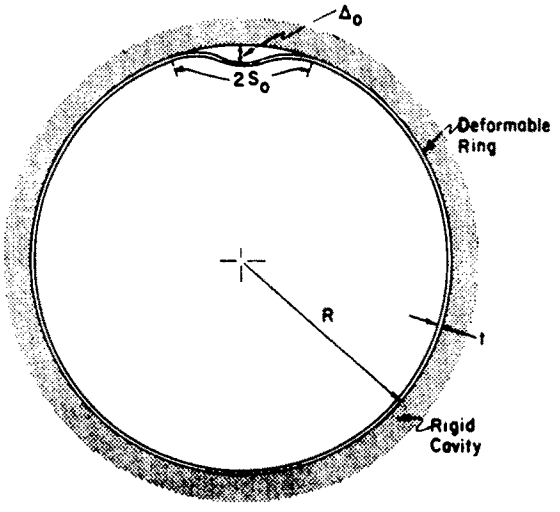

Fig. 2. Initial geometry of imperfect confined ring.

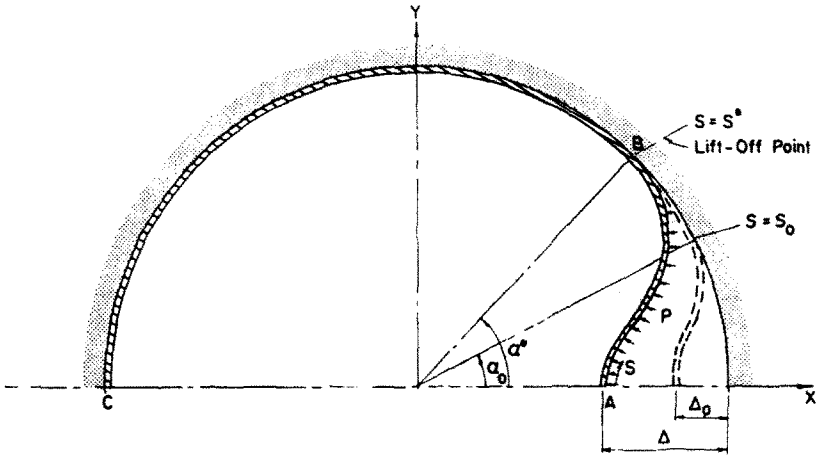

Fig. 3. Deformed configuration of a confined ring which has an initial imperfection.

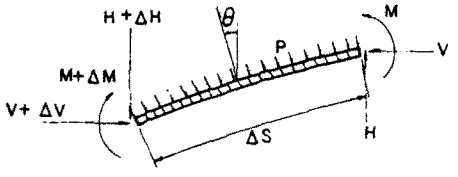

Fig. 4. Equilibrium of an elemental segment of detached ring section.

where S is the measure of length along the perimeter of the deformed ring and θ is the local angle formed between the outward normal to the ring midsurface the X-direction (Fig. 4).

The initial imperfection used affects a length $2S_0$ and has initial amplitude Δ_0. The same shape function was used as in [18]. It represents an imperfection with only one point of inflection and with positive curvature at A (see the Appendix).

Equilibrium equations

The equilibrium equations can easily be derived from Fig. 4 as:

$$\begin{aligned} \frac{dH}{dS} &= -P\cos\theta, \\ \frac{dV}{dS} &= -P\sin\theta, \\ \frac{dM}{dS} &= H\cos\theta + V\sin\theta, \\ \frac{dP}{dS} &= 0. \end{aligned} \tag{2}$$

Constitutive behavior

Both elastic and inelastic material behavior for the ring are considered. The constitutive equations are simplified considerably by considering only bending deformations and stresses. This is a reasonable assumption for relatively thin rings for which the mean stress

through the thickness is only a small fraction of the material yield stress. The stress–strain behavior of the ring is approximated with linear segments as shown in Fig. 5(a). For plastic behavior an intermediate hardening rule is used. The thickness integrated stress–strain relationships yield the following moment-curvature relationships:

$$\bar{M} = M(\alpha, \bar{\kappa}, \bar{\kappa}_1), \tag{3}$$

where

$$\bar{M} = 6M/\sigma_0 t^2, \quad \bar{\kappa} = \kappa t E/2\sigma_0 \text{ and } \alpha = E/E'; \tag{4}$$

the local curvature $\kappa(S)$ is given by:

$$\kappa(S) = \frac{d\theta_0}{dS} - \frac{d\theta}{dS}, \tag{5}$$

where $d\theta_0/dS$ is the curvature of the undeformed configuration. $\bar{\kappa}_1$ is a history dependent parameter necessary for plastically deformed sections and represents the maximum value of curvature reached by that section (see Fig. 5b). For strictly linear elastic material behavior (3), reduces to:

$$\bar{M} = \bar{\kappa}. \tag{6}$$

For nonlinear elastic behavior (3) becomes

$$\bar{M} = \bar{M}(\alpha, \bar{\kappa}). \tag{7}$$

This is represented by $OABF$ in Fig. 5(b) for both loading and unloading. Complete expressions for eqns (3), (6) and (7) have been presented in [13]. Reference [23] has extended these to include isotropic and kinematic hardening rules.

Equations (1)–(5) non-dimensionalized in the way shown below become:

$$\begin{aligned}
\frac{dx}{ds} &= -\sin\theta, \\
\frac{dy}{ds} &= \cos\theta, \\
\frac{d\bar{H}}{ds} &= -p\cos\theta, \qquad 0 \le s \le s^* \\
\frac{d\bar{V}}{ds} &= -p\sin\theta, \qquad s_0 \le s^* \le 1
\end{aligned} \tag{8}$$

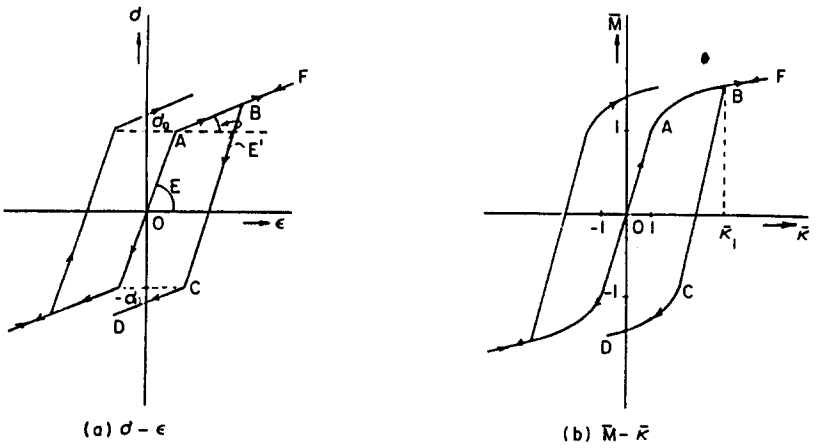

(a) $\sigma - \epsilon$ (b) $\bar{M} - \bar{\kappa}$

Fig. 5. Constitutive relationships.

$$\frac{d\bar{M}}{ds} = \bar{H}\cos\theta + \bar{V}\sin\theta,$$

$$\frac{dp}{ds} = 0,$$

$$\frac{d\theta}{ds} = \frac{d\theta_0}{ds} - 2\pi\left(\frac{R}{t}\right)\left(\frac{\sigma_0}{E}\right)\bar{\kappa}(\alpha, \bar{M}, \bar{\kappa}_1),$$

where

$$s = S/\pi R, \qquad x = X/\pi R, \qquad y = Y/\pi R,$$
$$\bar{H} = 6\pi RH/\sigma_0 t^2, \qquad \bar{V} = 6\pi RV/\sigma_0 t^2, \tag{9}$$
$$\bar{M} = 6M/\sigma_0 t^2, \qquad p = 6\pi^2\left(\frac{R}{t}\right)^2\frac{P}{\sigma_0}.$$

Boundary conditions

If the length of the detached section of the ring is prescribed to be s^*, then the point of liftoff from the wall can be defined by an angle $\alpha^* = s^*$. At this point continuity of displacement, slope and curvature are required leading to the development of a concentrated shear force. Using these assumptions and symmetry conditions at $s = 0$ the following boundary conditions must be satisfied by the solution

$$\begin{aligned} &\bar{H}(0) = 0, && \bar{M}(s^*) = 0, \\ &\theta(0) = 0, && \theta(s^*) = \alpha^*, \\ &y(0) = 0, && x(s^*) = (\cos\alpha^*)/\pi, \\ & && y(s^*) = (\sin\alpha^*)/\pi. \end{aligned} \tag{10}$$

Equations (8)–(10) constitute a two point boundary value problem which is solved numerically. The solution procedure involved expressing (8) in a forward difference form and solving the resulting nonlinear algebraic equations numerically using Newton's method. The interval $s\epsilon[0, s^*]$ was descritized into N points. An incremental type of solution procedure was used where the problem domain s^* was gradually increased and for each new value the solution was seeked.

The solution procedure started by increasing the initially detached length s_0 by Δs; thus $s^* \rightarrow s_0 + \Delta s$. The first initial guess was provided by guessing the value of the pressure p and based on this approximate value for the other variables were obtained using simple curved beam theory. For all subsequent increments of s^* the solution for the preceding configuration, suitably extended, was used as initial guess. This solution process was

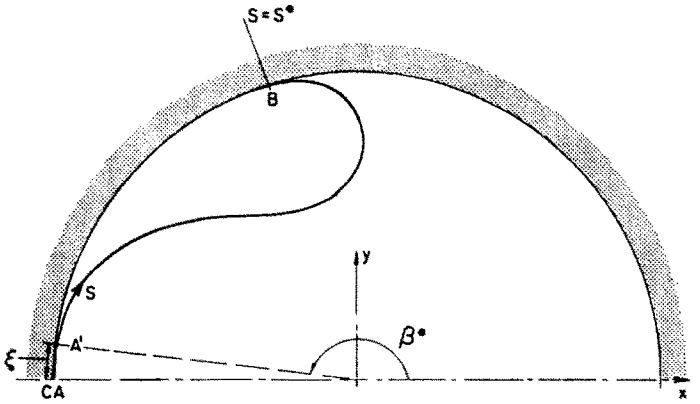

Fig. 6. Problem geometry after first touchdown.

repeated until the ring collapsed to a point where the crown of the ring touched the opposite wall for the first time. For the solutions beyond this point the boundary value problem solved had to be modified to accommodate the new contact area that develops around point A. It was assumed that further deformation will force part of the ring to come into contact with the opposite wall and conform to the circular shape of the wall as shown in Fig. 6. In addition, the thickness of the ring walls is neglected and both sections of the ring along AA' are assumed to be one radius away from the undeformed ring center.

The problem becomes one degree more difficult because in the configuration shown in Fig. 6 in addition to not knowing the position of point B, the position of point A' is also unknown. This difficulty was resolved as follows. We start by prescribing the length of the section of the ring that has touched the opposite side (i.e. the length of AA') as ξ. Thus, the boundary conditions at A' become:

$$\begin{aligned} &x(\xi) = (\cos\beta^*)/\pi, \\ &y(\xi) = (\sin\beta^*)/\pi, \qquad \text{where } \beta^* = (1-\xi)\pi, \\ &\theta(\xi) = \beta^*, \\ &\bar{M}(\xi) = \bar{M}(\hat{\kappa}(\xi)); \qquad \hat{\kappa}(\xi) = \frac{\mathrm{d}\theta_0(\xi)}{\mathrm{d}s} + \pi. \end{aligned} \tag{11a}$$

Although the position of point B is not known, it is known that the boundary conditions at that point should be

$$\begin{aligned} &\bar{M}(s^*) = 0, \\ &\theta(s^*) = \alpha^*, \qquad\qquad \alpha^* = s^*\pi \\ &x(s^*) = (\cos\alpha^*)/\pi, \\ &y(s^*) = (\sin\alpha^*)/\pi, \end{aligned} \tag{11b}$$

where the value of s^* remains an unknown. We proceed by guessing a value for s^* (usually take it to be equal to its value in the previous converged solution). This fixes the problem domain and the values of (11b). However, to avoid overdetermining the problem, one boundary condition has to be relaxed. The first of (11b) was chosen as the most suitable, thus, $\bar{M}(s^*) = 0$ is not enforced during the iterative solution. Thus, (8) with (11a and 11b) are solved as before. After a converged solution is obtained, the value of $\bar{M}(s^*)$ is compared to zero. Typically $\bar{M}(s^*) \neq 0$. With all other variables the same a new value of s^* is selected and the problem solved again. This procedured continues until the value of $\bar{M}(s^*)$ satisfies the zero condition to a predecided tolerance. By using the method of "false position" the number of iteration for convergence to the correct value of s^* was 3–5. Further collapse of the ring was achieved by increasing the value of ξ by $\Delta\xi$ and repeating the procedure. It must be emphasized that due to the nature of the problem, convergence was found to be very sensitive to the choice of increments of s^* before touchdown and of ξ after touchdown. An indication of the difficulties involved will be given in the next section.

RESULTS AND DISCUSSION

(a) *Linearly elastic case*

We first consider a material with linearly elastic constitutive behavior (represented by (6)). Equations (8)–(10) were solved using the procedure described above. The pressure v's change in volume response of the ring with a given imperfection is shown in Fig. 7. The response is characterized by a sharp rise to a limit load and a sharp drop down to a relatively low pressure "plateau" at which most of the deformation takes place. The limit load can be considered as the collapse pressure of the ring with the given imperfection. The response of the ring becomes unstable beyond this point. The limit load is strictly a function of the initial imperfection and this dependence is examined in more detail below.

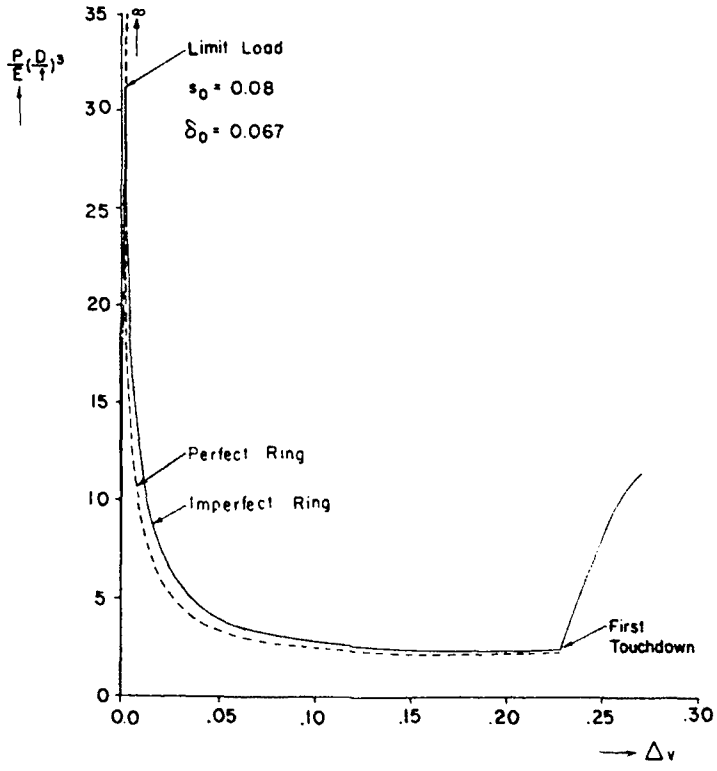

Fig. 7. Pressure v's volume change (linearly elastic case).

For a ring with no initial imperfection the response's stable branch (pressure axis) and the unstable branch only meet a ∞, as the response does not exhibit bifurcation points. The response for the perfect case is also plotted in Fig. 7. Comparison between the response of the perfect and imperfect geometries indicates that for larger deformations the effect of the imperfection on the response is small.

After first touchdown the ring response becomes again stable. This can be explained by the fact that the ring section is now supported at both ends, A and B in Fig. 6.

Due to the sharp rise to and sharp descent from the limit load exhibited by the response, the solution convergence around the limit load becomes very sensitive to the increment of S^* applied. A very fine descritization of the initial imperfection and a very gradual increase of s^* in the vicinity of the limit load were necessary. The unstable part of the response did not exhibit any numerical difficulties. After point A touched the opposite wall eqn (8) with boundary conditions (11) were solved according to the modified procedure described above. The solution was again very sensitive to the increment of ξ used. It was found necessary to introduce an auxilliary step in which the curvature at $\xi = 0$ was reduced in three steps from its value at first contact to the final value of $-1/R$. The procedure was continued by gradually incrementing ξ. It was observed that for the elastic case, point B started receding back up the cavity wall in essence decreasing s^*.

After a small touching segment was established, a third touchdown point developed somewhere between A' and B. Configurations beyond this point were not attempted. A set of ring collapse configurations including a few after touchdown, are shown in Fig. 8.

A limited study of the dependence of the response on the initial imperfections was carried out by varying the imperfection parameters δ_0 and s_0. Figure 9 shows a family of response curves (pressure v's crown displacement) where s_0 was kept constant and δ_0 varied between 0.0067 and 0.0112. The limit load is seen to be affected by the value of δ_0, but the remainder of the response are seen to coalesce to a common value. The variation of the detouched length with pressure for the same set of parameters is shown in Fig. 10.

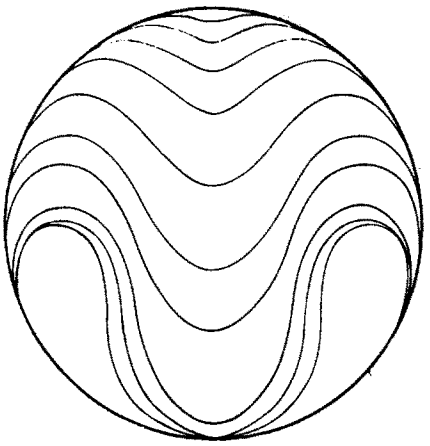

Fig. 8. Confined ring collapse configuration sequence (linearly elastic case).

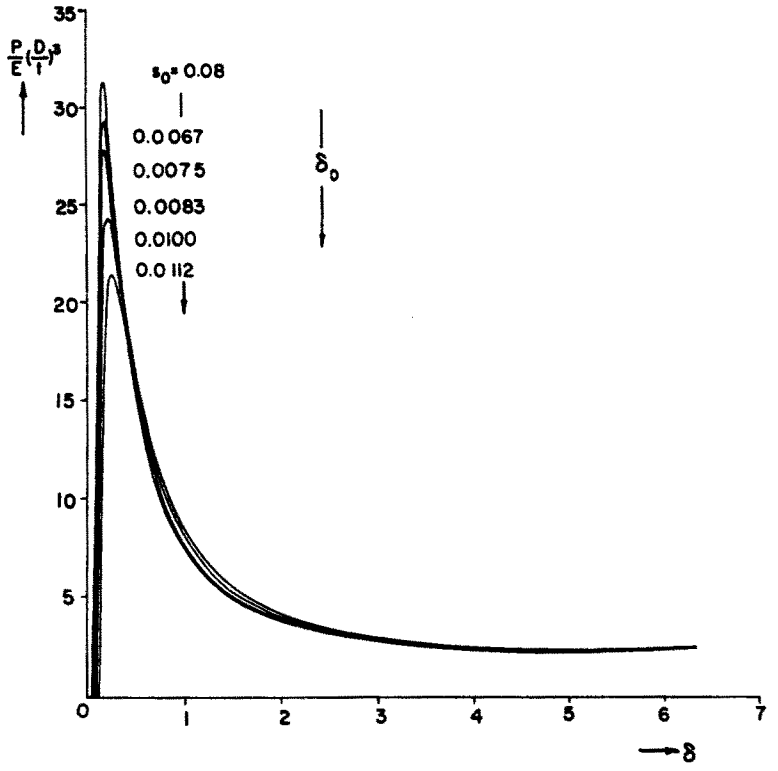

Fig. 9. Pressure v's crown displacement (linearly elastic case) for different values of δ_0.

Due to the nature of imperfection used, the range of imperfection amplitude (δ_0) that can be achieved for a fixed imperfection length (s_0) is limited. For this reason both parameters had to be varied in order to achieve a broad enough study of the imperfection sensitivity of the limit load. The results of this study are summarized in Fig. 11 where the limit load is plotted as a function of δ_0 for a range of values of s_0. The discontinuous results have been bounded with an envelope that might prove useful for design purposes. Note that for small values of both s_0 and δ_0 the limit load tends to increase substantially. For large enough parameters the limit load tends to a relatively constant value. The sensitivity of the limit load to the choice of imperfection shape made was not examined.

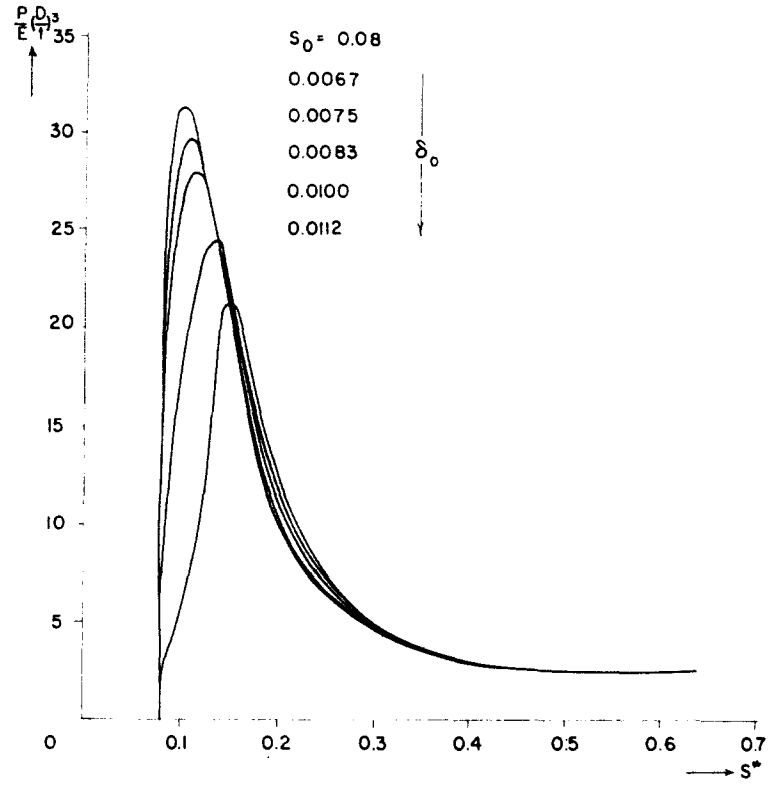

Fig. 10. Pressure v's separated length (linearly elastic case) for different values of δ_0.

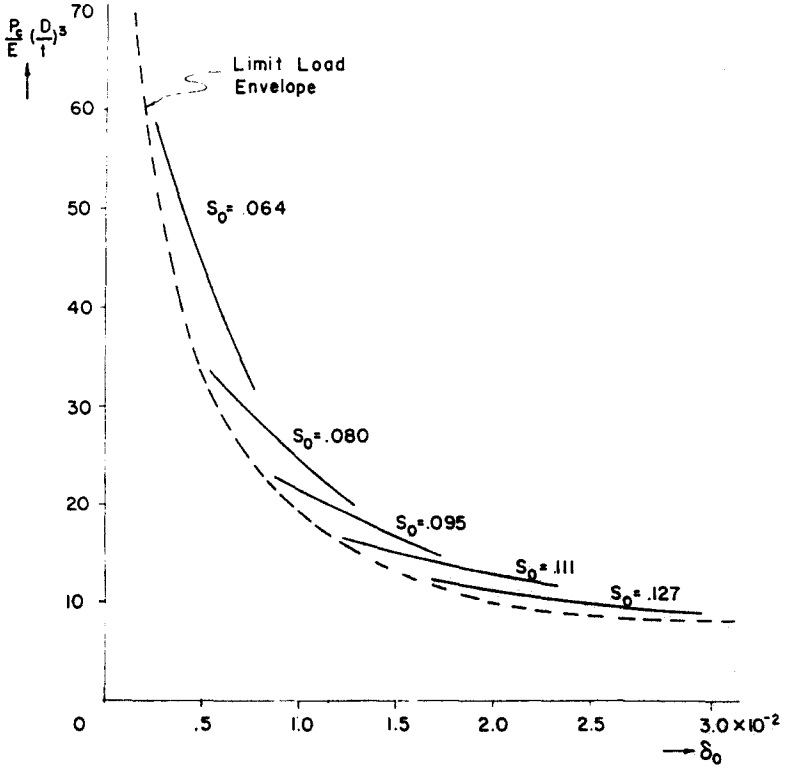

Fig. 11. Limit load for different magnitudes of imperfection and approximate limit load envelope (linearly elastic case).

(b) *Nonlinear elastic case*

Nonlinear elastic material behavior was also modeled by a bilinear stress–strain curve as shown in Fig. 5. For such a material both loading and unloading are assumed to occur along the same path. The constitutive equations for this material are

$$\bar{M} = \bar{\kappa} \quad \text{for } \bar{\kappa} \leq 1$$

$$\bar{M} = \frac{1}{\alpha}\bar{\kappa} - \frac{1}{2}\left(1 - \frac{1}{\alpha}\right)\frac{1}{\bar{\kappa}^2} + \frac{3}{2}\left(1 - \frac{1}{\alpha}\right) \quad \text{for } \kappa > 1.$$

The solution procedure used was similar to the one described in the previous section. The nature of the response has the same main characteristics (limit load, pressure plateau, etc.) as the elastic case. Convergence of the iterative solution scheme used was found to be more sensitive to the size of the domain increment Δs (the control parameter of the solution procedure) around the limit load. In addition, for higher values of α the growth of the detached section of ring almost ceases close to touchdown. As a result, using s^* as the control parameter was not very convenient. For this reason, the crown depth S was used as the control parameter for part of the response. This required a procedure similar to the one described above for the response of the ring beyond first touchdown.

Figure 12 shows a family of responses for different values of the strain hardening parameter α. The value of the limit load is very sensitive to the value of α when α is close to 1. The limit load decreases sharply as α increases from 1 and becomes almost insensitive to the value of α when α reaches around 80 and beyond. Looking at the minimum loads reached by the curves, it can be seen that the minimum loads are also affected by the value of α. In Fig. 13 the parameter σ_0/E is varied. The effect of higher yield stress is to increase both the limit and minimum loads of the response.

Elastic–plastic case

Elastic–plastic material behavior differs from the nonlinear elastic model described above in that it allows for elastic unloading and permanent deformation of the material.

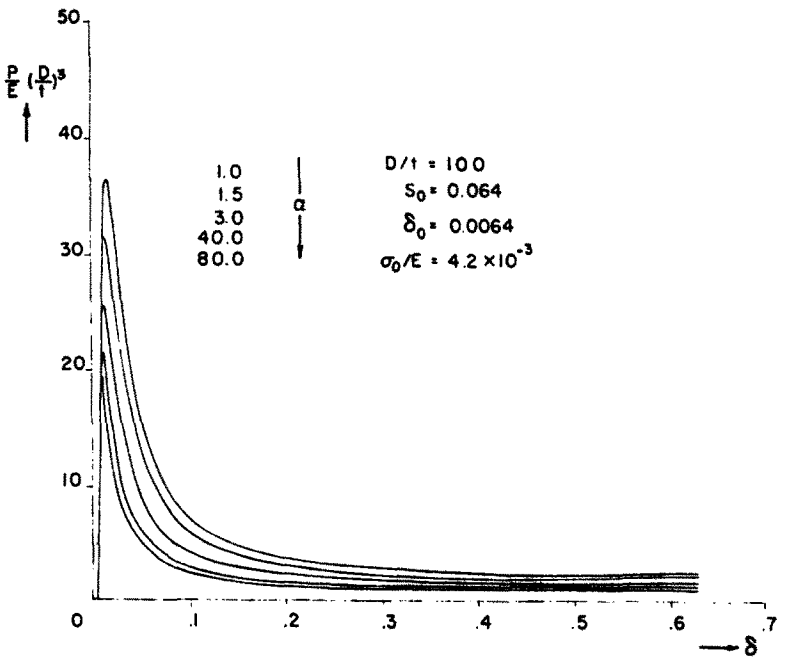

Fig. 12. Pressure v's crown displacement for different values of strain hardening (non-linear elastic case).

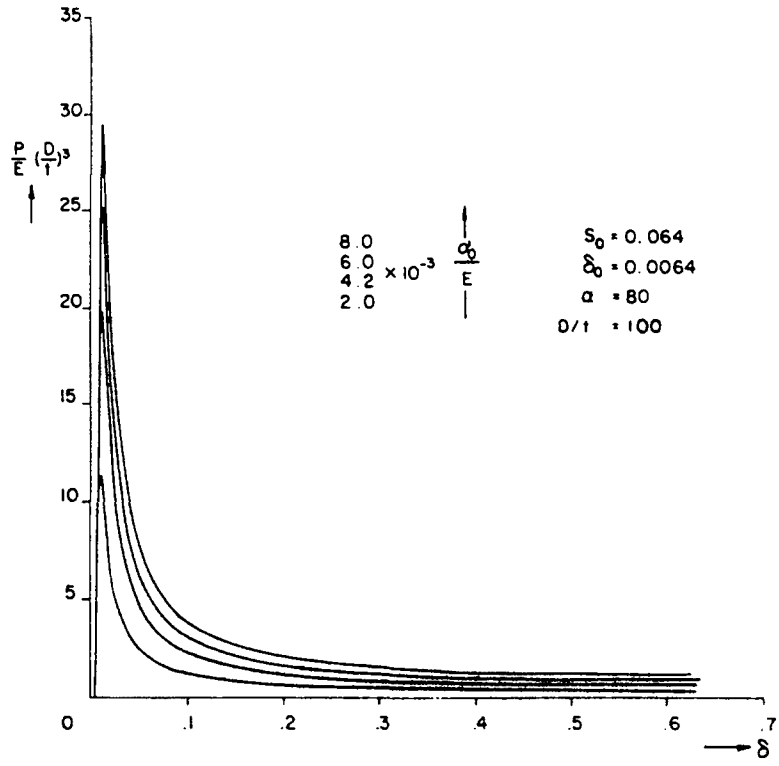

Fig. 13. Pressure v's crown displacement for different values of σ_0/E (non-linear elastic case).

The constitutive relations used are represented by (3) and (4), (the equations have been developed in [13]). The solution procedure is basically the same as in the case of the nonlinear elastic problem. However, much bigger computer memory is required as all previous solutions are stored in order to compare with the current one. During the iterative procedure, the moment at every nodal point is compared to that of the previous converged solution at the same point. If the moment is found to be greater than the one from the previous equilibrium state, the constitutive law based on OAF (Fig. 5b) is used. If not, the point is undergoing unloading, thus it is forced to follow the path ABC. If a point first undergoes unloading and then is subjected to reloading before it reached C, it is forced to return back along CBF. Since the path ABC depends on the point of unloading, B, the value of curvature at β, $\bar{\kappa}_1$, is stored and is updated if it changes. In some of the cases considered, the direction of bending changed more than once in which case the same reverse loading procedure described above was applied to points along BCD.

A typical response obtained for this type of material behavior is shown in Fig. 14. The main characteristics of the response are unchanged. However, the convergence of the iterative scheme became even more sensitive to the size of domain increment Δs. As in the elastic cases, very small size of increment was required to locate the limit load. If too large an increment was used, the equilibrium would jump from the stable to the unstable branch without going through the limit load. Difficulty in convergence also occurred for values of s^* over 0.6. In this vicinity the size of increments used was as small as 1/30–1/150 of that used in the linearly elastic case. As a result, the solution procedure was much slower. For this reason the alternate procedure of incrementing δ instead of s^* proved more time efficient in spite of having to deal with two nested iterations.

The response obtained for the elastic–plastic case is compared with the corresponding responses for the two elastic cases considered in Fig. 14. The elastic–plastic case and nonlinearly elastic cases have very similar responses before and close to the limit load. This is to be expected because at this early stage no material unloading has yet developed. As the deformations grow the elastic–plastic response becomes stiffer than the nonlinear

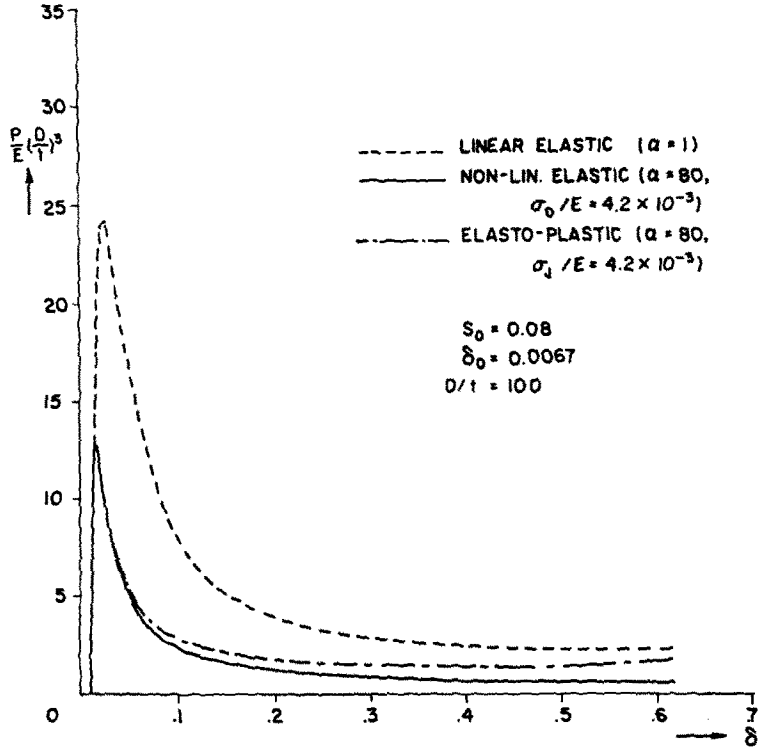

Fig. 14. Pressure v's crown displacement for different material models.

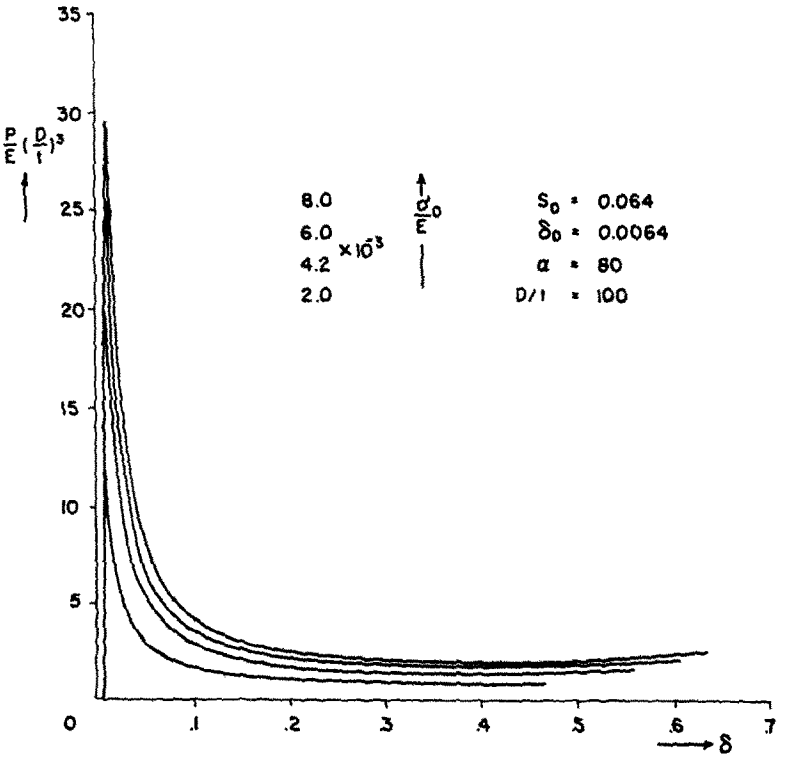

Fig. 15. Pressure v's crown displacement for different values of σ_0/E (elastic–plastic case).

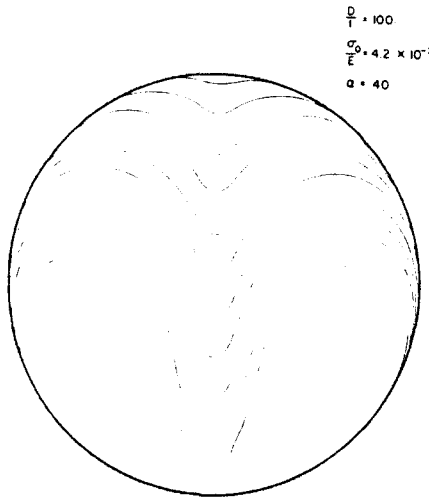

Fig. 16. Collapse sequence (elastic–plastic case).

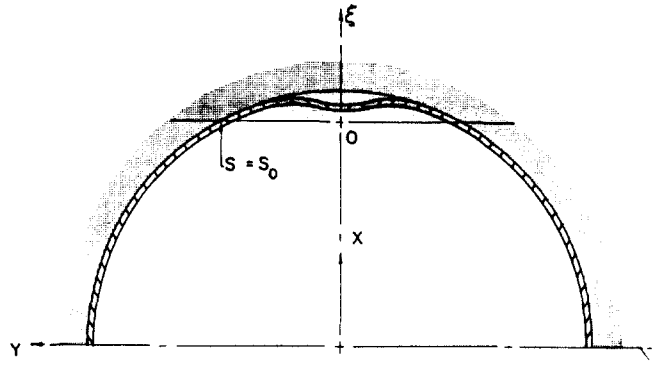

Fig. 17. Coordinates of imperfection ($S - \xi$).

elastic case. This is due to the hardening that sections of the deformed ring undergo as a result of reverse bending. The linearly elastic case plotted on the same figure exhibits a substantially higher limit load and a much higher postbuckling collapse pressure.

A family of responses for different values of σ_0/E for the elastic–plastic material are plotted in Fig. 15. The value of σ_0/E is varied from 2.0×10^{-3} to 8.0×10^{-3} with all other parameters kept constant. It is clear that the value of σ_o/E affects both the limit load as well as the remainder of the large deflection response. The effect of the material on the collapse configurations is shown in Fig. 16. If compared with the ones presented for the elastic case (Fig. 8) the crown of the deforming ring is found to undergo more extreme deformations in the case of this material.

CONCLUSIONS

The large deflection response of thin-walled confined rings under external pressure has been obtained numerically. The ring has been assumed to remain inextensional. This step is crucial for the kinematics of the ring assumed. It is however restrictive as to the range of D/t that the analysis can be applied to. The response of the ring under external pressure was found to be characterized by a limit load and an unstable post limit load response until the deformation caused points on the ring walls to come into contact after which the path became stable again. The characteristics of the response are retained for linearly elastic, nonlinear elastic and elastic–plastic material models.

Acknowledgements—The work presented was supported in part by the National Science Foundation under grant CEE-81-05539 and by the University of Texas at Austin. Their support is greatly appreciated. The authors would also like to express their thanks to Ms. M. L. Aiken for typing the manuscript and to Mr. V. Toth for photographic assistance.

REFERENCES

1. H. G. Texter, Oil-well casing and tubing troubles. *Drilling and Production Practice (API)*, pp. 7–51 (1955).
2. T. Ahrens, An in-depth analysis of well casings and grouting: Basic considerations of well design—II. *Water Well J.*, 49–51 (1970).
3. I. W. McCaig and P. J. Folberth, The buckling resistance of steel liners for circular pressure tunnels. *Water Power* **14**, 272–278 (1962).
4. F. Ullamn, External water pressure designs for steel-lined pressure shafts. *Water Power* **16**, 298–305 (1964).
5. Y. Yamamoto and N. Matsubara, Buckling of a cylindrical shell restrained by an outer rigid wall. *Theor. Appl. Mech. (Japan)* **27**, 115–126 (1977).
6. Y. Yamamoto and N. Matsubara, Buckling strength of steel cylindrical liners for waterway tunnels. *Theor. Appl. Mech. (Japan)* **30**, 225–235 (1981).
7. S. Kyriakides, Propagating buckles in long cylindrical confined shells. *EMRL Rep. No.* 84/4, U.T. Austin.
8. R. Montel, A semi-empirical formula for determining the limiting external pressure for the collapse of smooth metal pipes embedded in concrete. La Houille Blanche, No. 5, pp. 560–569 (Sept.–Oct. 1960).
9. E. Amstutz, Das Einbeulen von Schacht—und Stollenpanzerungen. *Schweizerische Bauzeitung* **87**, 541–549 (1969).
10. S. Kyriakides and C. D. Babcock, Buckle propagation phenomena in pipelines. Collapse: The buckling of structures in theory and practice. *Proc. IUTAM Symp. on Collapse*, London, Aug. 1982 (Edited by J. M. T. Thomson and G. W. Hunt), pp. 75–91. Cambridge University Press (1983).
11. S. Kyriakides and C. D. Babcock, Experimental determination of the propagation pressure of circular pipes, *J. Pressure Vessel Tech., Trans. ASME* **103**, 328–336 (1981).
12. S. Kyriakides and C. D. Babcock, Large deflection collapse analysis of an inelastic inextensional ring under external pressure. *Int. J. Solids Structures* **17**, 981–993 (1981).
13. S. Kyriakides and E. Arikan, Postbuckling behavior of inelastic inextensional rings under external pressure. *J. Appl. Mech., Trans. ASME*, (Sept. 1983).
14. E. Chater and J. W. Hutchinson, On the propagation of bulges and buckles. Harvard University Rep. MECH-44 (June 1983).
15. S. Kyriakides, M-K. Yeh and D. Roach, On the determination of the propagation pressure of long cylindrical tubes, *J. Pressure Vers. Tech., ASME*, in press (1984).
16. Hsu Lo, J. L. Bogdanoff, J. E. Goldberg and R. F. Crawford, A buckling problem of a circular ring. *Proc. 4th U.S. Nat. Congr. Appl. Mech., ASME* **1**, 691–695 (1962).
17. R. T. Hsu, J. Elkon and T. H. H. Pian, Note on the instability of circular rings confined to a rigid boundary. *J. Appl. Mech., Trans. ASME*, 559–562 (1964).
18. L. L. Bucciarelli, Jr. and T. H. H. Pian, Effect of initial imperfections on the instability of a ring confined in an imperfect rigid boundary. *J. Appl. Mech., Trans. ASME*, 979–984 (1964).
19. H. C. Chan and S. J. McMinn, The stability of a uniformly compressed ring supported by a rigid circular surface. *Int. J. Mech. Sci.* **8**, 433–442 (1966).
20. E. A. Zagustin and G. Herrmann, Stability of an elastic ring in a rigid cavity. *J. Appl. Mech., Trans. ASME*, 263–270 (1967).
21. L. El-Bayoumy, Buckling of a circular elastic ring confined in a uniformly contracting circular boundary. *J. Appl. Mech., Trans. ASME*, 758–766 (1972).
22. T. J. Lardner, On the nonbuckling of a circular ring under a wrapping load. *J. Appl. Mech., Trans. ASME* **47**, 973–974 (1980).
23. S.-K. Youn, Large deflection collapse analysis of a circular confined ring under external pressure. M.S. Thesis, Department of Aerospace Engng and Engng Mech., U.T. Austin, *EMRL Rep. No.* 83/2 (Aug. 1983).

APPENDIX

The imperfection shape function used is the same as the one developed in [18]. It is symmetric about the x-axis and is assumed to be formed inextensionally from the perfectly circular ring geometry. The imperfection is defined through the following expressions (see Fig. 17).

$$\frac{d\xi^2}{dS^2} = \frac{1}{R}\left\{\beta\left[\cos\left(4.493\frac{S}{S_0}\right) - \cos 4.493\right] - 1\right\} \qquad S \le S_0$$
$$\frac{d\xi}{dS} = \frac{S_0}{R}\left\{-\frac{S}{S_0} + \frac{\beta}{4.493}\left[\sin\left(4.493\frac{S}{S_0}\right) - 4.493\frac{S}{S_0}\cos 4.493\right]\right\} \tag{A1}$$

where S_0 and β are the two parameters that can be varied. $2S_0$ represents the length of the ring affected by imperfection. β must be bigger than 0.822 in order to have a change in sign of curvature along the length of the imperfection. In the notation developed in the paper

$$\frac{d\theta_0}{dS} = \frac{\dfrac{d^2\xi}{dy^2}}{\left[1 + \left(\dfrac{d\xi}{dY}\right)^2\right]^{3/2}}. \tag{A2}$$

which can be obtained from (A1).